Multivariate classification provides a neural signature of Tourette disorder

Giuseppe A. Zito[1,2] (iD), Andreas Hartmann[1,3], Benoît Béranger[4], Samantha Weber[5], Selma Aybek[5], Johann Faouzi[6], Emmanuel Roze[1], Marie Vidailhet[1] and Yulia Worbe[1,3,7]

[1]Sorbonne University, Inserm U1127, CNRS UMR7225, UM75, Paris Brain Institute, Movement Investigation and Therapeutics Team, Paris, France; [2]Support Centre for Advanced Neuroimaging (SCAN), University Institute of Diagnostic and Interventional Neuroradiology, Inselspital, Bern University Hospital, University of Bern, Freiburgstrasse, Bern CH-3010, Switzerland; [3]National Reference Center for Tourette Syndrome, Assistance Publique-Hôpitaux de Paris, Groupe Hospitalier Pitié-Salpêtrière, Paris, France; [4]Center for NeuroImaging Research (CENIR), Paris Brain Institute, Sorbonne University, UPMC Univ Paris 06, Inserm U1127, CNRS UMR, 7225, Paris, France; [5]Psychosomatics Unit of the Department of Neurology, Inselspital, Bern University Hospital, University of Bern, Freiburgstrasse, Bern CH-3010, Switzerland; [6]Sorbonne University, Inserm U1127, CNRS UMR7225, UM75, ICM, Inria Paris, Aramis project-team, Paris, France and [7]Department of Neurophysiology, Saint-Antoine Hospital, Assistance Publique-Hôpitaux de Paris, Paris, France

Abstract

Background. Tourette disorder (TD), hallmarks of which are motor and vocal tics, has been related to functional abnormalities in large-scale brain networks. Using a fully data driven approach in a prospective, case–control study, we tested the hypothesis that functional connectivity of these networks carries a neural signature of TD. Our aim was to investigate (i) the brain networks that distinguish adult patients with TD from controls, and (ii) the effects of antipsychotic medication on these networks.
Methods. Using a multivariate analysis based on support vector machine (SVM), we developed a predictive model of resting state functional connectivity in 48 patients and 51 controls, and identified brain networks that were most affected by disease and pharmacological treatments. We also performed standard univariate analyses to identify differences in specific connections across groups.
Results. SVM was able to identify TD with 67% accuracy ($p = 0.004$), based on the connectivity in widespread networks involving the striatum, fronto-parietal cortical areas and the cerebellum. Medicated and unmedicated patients were discriminated with 69% accuracy ($p = 0.019$), based on the connectivity among striatum, insular and cerebellar networks. Univariate approaches revealed differences in functional connectivity within the striatum in patients *v.* controls, and between the caudate and insular cortex in medicated *v.* unmedicated TD.
Conclusions. SVM was able to identify a neuronal network that distinguishes patients with TD from control, as well as medicated and unmedicated patients with TD, holding a promise to identify imaging-based biomarkers of TD for clinical use and evaluation of the effects of treatment.

Introduction

Tourette disorder (TD) is a neurodevelopmental disorder characterized by motor and vocal tics (American Psychological Association, 2013). It is often associated with psychiatric comorbidities, of which obsessive–compulsive disorders (OCDs), attention-deficit hyperactivity disorders (ADHDs), intermittent explosive disorders (IEDs) and depression represent the most common ones (Hirschtritt et al., 2015).

A dysfunction of cortico-striato-thalamo-cortical (CSTC) loops might account for this clinical spectrum (Singer, 2005), as structural and functional abnormalities have been found in the basal ganglia (Worbe et al., 2010, 2012), the sensory-motor areas (Fahim et al., 2010; Worbe et al., 2010), the dorsolateral prefrontal cortex and more generally the frontal cortex (Fredericksen et al., 2002; Kates et al., 2002), fronto-parietal networks (Atkinson-Clement et al., 2020; Eddy, Cavanna, Rickards, & Hansen, 2016) and the cerebellum (Lerner et al., 2007). Some of these abnormalities have been related to the disorder itself, but others have been associated with comorbidities, as well as with compensatory strategies to reduce the tics (Mazzone et al., 2010). Despite an extensive research, no reliable brain biomarker of this disorder has been found, and the precise pathophysiological mechanisms of TD are still poorly understood.

Multivariate approaches applied to neuroimaging, such as functional magnetic resonance imaging (fMRI), represent a valuable method to address the complex aspects of TD, due to

Table 1. Clinical and demographic data

	HC (N = 51)	TD (N = 48)	Statistics	TD without medication (N = 18)	TD with medication (N = 18)	Statistics
Sex (male/female)	33/18	38/10	$\chi(1) = 2.55$, $p = 0.110$	14/4	13/5	$\chi(1) = 0.15$, $p = 0.700$
Age (years, mean ± s.d.)	30.9 ± 10.4	30.5 ± 10.3	$t(97) = 2.11$, $p = 0.833$	30.7 ± 11.2	31.4 ± 9.5	$t(34) = 0.21$, $p = 0.836$
YGTSS50	–	16.5 ± 7.2	–	15.5 ± 8.0	17.11 ± 6.0	$t(34) = 0.68$, $p = 0.498$
IED [N (% of TD)]	–	22 (45.8%)	–	50%	38.9%	$\chi(1) = 0.45$, $p = 0.502$
ADHD [N (% of TD)]	–	20 (41.7%)	–	38.9%	27.8%	$\chi(1) = 0.50$, $p = 0.480$
OCD [N (% of TD)]	–	10 (20.8%)	–	11.1%	16.7%	$\chi(1) = 0.23$, $p = 0.630$
Overall medication [N (% of TD)][a]	–	18 (37.5%)				
Aripiprazole, APZ [N (% of TD)]	–	15 (31.2%)				
Topiramate [N (% of TD)]	–	2 (4.2%)				
Fluoxetine [N (% of TD)]	–	2 (4.2%)				
Risperidone [N (% of TD)]	–	2 (4.2%)				
Others (pimozide, escitalopram, haloperidol, mianserin – [N (% of TD)])	–	4 (8.3%)				

YGTSS, Yale global tic severity score; IED, intermittent explosive disorder; ADHD, attention deficit hyperactivity disorder; OCD, obsessive–compulsive disorder; HC, healthy control; TD, Tourette disorder.
Comparison of clinical and demographic scores across groups.
[a]All medications were prescribed for at least 3 years.

their ability to (i) detect subtle and distributed patterns of activity throughout the brain in a fully data-driven manner, (ii) make predictions that have the potential to interrogate neurophysiological mechanisms, and (iii) aid in diagnosis and treatment (Nielsen, Barch, Petersen, Schlaggar, & Greene, 2019). Recent studies have used multivariate approaches, in particular support vector machine (SVM), to discriminate children with TD from age-matched healthy controls (HCs) (Greene et al., 2016), as well as young TD patients from older ones (Nielsen et al., 2020). They have shown that functional brain abnormalities allow for the identification of TD with ~70% accuracy, and that delayed brain maturation may explain the atypical functional connectivity in adults with TD. However, they did not search a neural signature of the disorder in relation to pharmacological treatment. This is relevant, as patients with TD are often treated with antipsychotics and, even if their effects on the symptoms are documented, their specific action on large-scale brain networks is still unknown (Handley et al., 2013).

We employed a multivariate approach to predict patterns of resting state functional connectivity (rs-FC) in TD which: (i) inform on the neurophysiological mechanisms of adult TD, (ii) address the differences between TD patients under antipsychotic medication and unmedicated ones and (iii) correlate with symptoms' severity. We applied SVM to identify differences in connectivity patterns between TD patients and HCs, as well as between patients with and without medication. We also implemented a support vector regression (SVR) model that investigates whether rs-FC carries information about symptoms' severity. In addition to SVM, we performed a standard univariate analysis to evaluate specific differences in rs-FC across groups.

Our ultimate goal was to shed light on the altered brain functions underpinning TD in adults, as well as their link to medication status, and to study the potential of SVM as a predictive tool to support the diagnosis of TD.

Materials and methods

Participants and general procedure

We recruited 55 patients with TD and 55 sex- and age-matched HCs. Seven patients and four HCs were not able to perform the MRI (due to e.g. excessive movements) and were excluded from the analysis. The final sample consisted of 48 patients with TD (39 male, mean age: 30.5 ± 10.3 years) and 51 HCs (33 male, mean age: 30.9 ± 10.4 years).

Patients were recruited through the National Tourette Disorder reference center at the Pitié-Salpêtrière Hospital in Paris. Inclusion criteria for patients were: a diagnosis of TD according to DSM-5 (American Psychological Association, 2013), capability to control tics for at least 10 min during the MRI acquisition. Exclusion criteria for both HCs and patients with TD were: incompatibility with MR acquisition (e.g. claustrophobia and metallic body implants), history of alcohol or drug addiction (except for nicotine and recreational cannabis use for less than once per week), history of psychosis and learning disability. We also excluded HCs who experienced childhood tics and any neurological disorders.

In patients, tic severity was assessed using the Yale Global Tic Severity Scale (YGTSS50) (Leckman et al., 1989). The life-long diagnosis of psychiatric comorbidities, such as OCDs, ADHDs and IEDs, typically observed in TD (Hirschtritt et al., 2015), was evaluated using patients' medical records and psychiatric evaluations available at the inclusion in the study. Eighteen patients with TD were under stable medication for at least 3 years at the time of examination (Table 1).

Standard protocol approvals, registrations and patients consent

The study was carried out in accordance with the latest version of the Declaration of Helsinki and approved by the local Ethics

Committee (approval number: CCP16163/C16-07). All participants gave written informed consent prior to the study. The study was registered in ClinicalTials.gov (ID number: NCT02960698).

Clinical groups' analysis

We performed two analyses investigating: (i) between-group differences in 51 HCs and 48 patients with TD, and (ii) between-TD patients' subgroup differences in 18 patients with medication and 18 patients without medication. For the latter, as SVM achieves best performance when the two discriminated groups contain the same number of samples (Wu & Chang, 2003), we analyzed data from all patients with TD under medication ($n = 18$) and a subset of 18 unmedicated patients that matched the group of medicated TD for age, sex, symptom severity and comorbidities. This ensured balanced groups, and excluded potential confounds due to between-group differences other than in rs-FC.

Differences in age were assessed with independent-sample t tests, whereas differences in the ratio between male and female participants were assessed with χ^2 tests. Moreover, for the between-TD patients' subgroup analysis, differences in the YGTSS50 were assessed with independent-sample t tests, and differences in the ratio of patients with and without IED, ADHD and OCD were assessed with χ^2 tests. The significance level was set at 0.05. Data analysis was performed with SPSS 25 (IBM Statistics, USA).

Neuroimaging acquisition parameters and pre-processing

During the MR session, participants were asked to lie still with the eyes open, while fixating a cross on a screen. Eye movements were monitored with an eye-tracking device. Neuroimaging data were acquired using a 3T Magnetom Prisma (Siemens, DE) with a 64-channel head coil. Resting state fMRI and structural images were acquired in one session using the following parameters: (i) echo-planar imaging sequences performed with a multi-slice, multi-echo acquisition, repetition time (TR) = 1.9 s, echo time (TE) = 17.2/36.62/56.04 ms, Ipat acceleration factor = 2, multiband = 2, isotropic voxel size = 3 mm, dimensions = 66×66 in plane $\times 46$ slices, 350 volumes, duration = 11 min; (ii) a T1-weighted MP2RAGE sequence with TR = 5 s, inversion time (TI) = 700/2500 ms, field of view (FOV) = 232×256 in plane $\times$ 176 slices, 1 mm isotropic, Ipat acceleration factor = 3.

T1-weighted images were first background denoised (O'Brien et al., 2014) using https://github.com/benoitberanger/mp2rage, which is based on Marques. This step improved the quality of the subsequent segmentation. Images were then pre-processed (segmentation, normalization to Montreal Neurological Institute – MNI – space) using the Computational Anatomy Toolbox (http://www.neuro.uni-jena.de/cat/) extension for SPM12 (https://www.fil.ion.ucl.ac.uk/spm/).

Functional data were pre-processed with AFNI using *afni_proc.py* script (https://afni.nimh.nih.gov/) according to standard procedures (despiking, slice timing correction and realignment to the volume with the minimum outlier fraction driven by the first echo). A brain mask was computed on the realigned shortest echo temporal mean using FSL BET (Jenkinson, Beckmann, Behrens, Woolrich, & Smith, 2012). This step increased the robustness against strong signal bias intensity. Afterward, the TEDANA toolbox (Kundu et al., 2017) version 0.0.7 was used to optimally combine the realigned echoes, to reduce the dimensionality of the dataset by applying principal component analysis,

and to perform an independent component analysis (ICA) decomposition which separated BOLD from non-BOLD components, based on the TE dependence of the ICA components (Kundu, Inati, Evans, Luh, & Bandettini, 2012). This step ensured robust artifact removal of non-BOLD components, such as movement, respiration or heartbeat. Previous research with resting state fMRI has already confirmed the superiority of this method in regressing out motion over standard denoising techniques (Kundu et al., 2017). To further confirm this, framewise displacement (FD) was computed according to standard methods (Power et al., 2014), and compared between the groups. No motion artifacts affected the quality of the signal, the FD in TD (0.016 ± 0.007 mm) did not statistically differ from HC (0.136 ± 0.006 mm) [$t(97) = 1.91$, $p = 0.059$], and FD in patients with medication (0.016 ± 0.009 mm) did not statistically differ from patients without medication (0.016 ± 0.005 mm) [$t(34) = 0.21$, $p = 0.830$]. Finally, using SPM12, images were co-registered to the anatomical scan, normalized to MNI space, then smoothed with a Gaussian kernel with full width at half maximum of $5 \times 5 \times 5$ mm.

Brain images were parcellated into 116 functional regions, based on the automatic anatomical labeling (AAL) atlas (Tzourio-Mazoyer et al., 2002), and the region-averaged time series were extracted. The first 10 time points were discarded to ensure magnetization equilibrium. Motion parameters and the average signal of white matter and cerebrospinal fluid obtained during the segmentation, were regressed out. Time series were finally band-pass filtered at $0.009 < f < 0.08$ Hz, according to previous studies (Greene et al., 2016; Nielsen et al., 2020). We computed pairwise Pearson correlation coefficients between all pairs of brain regions as indicators of their functional connectivity, and we obtained a symmetric correlation matrix of 116×116 coefficients for each participant, i.e. 6670 correlation coefficients. Next, we converted the correlation coefficients to z-scores using Fisher-Z transformation, in order to normalize them to a Gaussian distribution (Wegrzyk et al., 2018).

Multivariate analysis for neuroimaging data

The 6670 correlation coefficients were used as features for linear SVM models. We implemented three predictive models to: (i) distinguish HCs from patients with TD, (ii) distinguish patients with and without medication and (iii) predict symptoms' severity in patients with TD. The first two models were initially optimized with an automatic grid search algorithm based on Bayesian optimization (Hastie, Tibshirani, & Friedman, 2009). The optimization minimized the cross-validation loss (error) by iteratively varying the C parameter and Kernel Scale. In line with previous research (Nielsen et al., 2020; Wegrzyk et al., 2018), the best values were found to be $C = 1$ and Kernel Scale = 1. The models were then trained to learn a function that separates the two groups, based on the differences in their rs-FC. The models were trained on a known dataset of participants belonging to the two groups, and mathematically assigned weights to each connection, based on its contribution to the discrimination. Once the models were built, they used these weights to predict the group where a new and unknown participant belongs to. We applied leave-one-subject-out-cross-validation (LOSOCV) to estimate the generalization of the models. The statistical significance of the classification accuracy was assessed using its null distribution under permutation testing, where group labels were randomly permuted 1000 times. We finally trained the SVMs with all HCs and patients, and identified the most discriminative

Table 2. Results of the multivariate analysis

	Accuracy (%)	Specificity (%)	Sensitivity (%)	*p*-value
Between-group classifier (TD *v.* HC)	67	65	69	0.004
Between-TD patients' subgroup classifier (TD with *v.* without medication)	69	67	72	0.019

HC, healthy control; TD, Tourette disorder.
Predictive performance of the SVM classifiers. *p* values represent the significance of the results, compared to chance.

connections as the ones holding the highest weights (Wegrzyk et al., 2018). This step was performed after evaluating that the most discriminative connections obtained following training the SVM with the entire dataset were consistent with the ones calculated by the single LOSOCV folds (online Supplementary Fig. S1). We studied whether rs-FC contains information about symptom severity by implementing a SVR model [$C = \infty$, Kernel Scale = 1, $\epsilon = 0.00001$, according to previous research (Nielsen et al., 2020) and optimized with Bayesian optimization, as described above] to predict YGTSS50 (Greene et al., 2016), and estimated it with LOSOCV. We studied the performance of the SVR model with r^2. The SVM and SVR were implemented with the Statistics and Machine Learning Toolbox in Matlab R2018a (The MathWorks, USA).

Univariate analysis for neuroimaging data

We performed a standard univariate analysis to study specific differences in rs-FC across groups. We compared the 6670 correlation coefficients between HCs and patients with TD, and between patients with and without medication, respectively, with multiple independent *t* tests. Moreover, in patients with TD, we computed Pearson's correlation coefficients between each connection and the YGTSS50. All tests were corrected for multiple comparisons with 1000 permutations. The significance level was set to 0.05 after correction. Data analysis was implemented in Matlab R2018a.

Results

Subjects

No statistically significant differences were found in sex and age between TD and HC. No statistically significant differences were found in tic severity and in the occurrence of comorbidities between medicated and unmedicated patients. Demographic and clinical data are presented in Table 1.

Multivariate analysis of rs-FC between the groups

The performance of the first two classifiers is shown in Table 2. The classifiers discriminated TD from HC (*p* = 0.004), as well as TD with and without medication (*p* = 0.019), with accuracy, specificity and sensitivity well above chance.

For the between-group classification analysis, the SVM identified the most discriminative connections, i.e. the connections holding the highest weights, in fronto-cerebellar, fronto-parietal, parieto-cerebellar and subcortico-subcortical networks (Fig. 1a and online Supplementary Fig. S1A). In particular, Fig. 1a shows that the classification accuracy was driven by the connectivity between (i) the cerebellar lobule 7b and the superior parietal gyrus, (ii) the orbito-frontal cortex (OFC) and the angular gyrus,

(iii) the putamen and the caudate, (iv) the caudate and the cerebellar lobule 10 and (v) the cerebellar vermis 9 and the OFC (online Supplementary Table S1).

For the between-TD patients' subgroup classification analysis, the SVM identified the most discriminative connections in fronto-cerebellar, cerebello-limbic, parieto-cerebellar and cerebello-subcortical networks (Fig. 1b and online Supplementary Fig. S1B). Figure 1b shows that the performance of the classifier was driven by the connectivity (i) of the supplementary motor area (SMA) with the cerebellar lobule 7b and the supramarginal gyrus, respectively, (ii) within the cerebellar regions, namely between crus 2 and, respectively, 4th, 5th, and 10th lobules, (iii) between the right caudate and the right insula and (iv) between the cerebellum (vermis 9 and 9th lobule) and the OFC and the inferior frontal gyrus, respectively (online Supplementary Table S2). These patterns were independent of the number of top feature weights considered, as shown in online Supplementary Fig. S2.

The analysis of the SVR showed that rs-FC was not able to predict symptom severity in patients with TD ($r^2 = 0.05$, *p* = 0.114).

Univariate analysis of rs-FC

The univariate analysis showed increased functional connectivity, in patients with TD compared to HCs (Fig. 2a), of the right caudate with the right and left putamen, respectively [$t(97) = 5.06$, $p_{corrected} = 0.003$ and $t(97) = 5.29$, $p_{corrected} = 0.001$], and of the left caudate with the right and left putamen, respectively [$t(97) = 4.21$, $p_{corrected} = 0.050$ and $t(97) = 4.38$, $p_{corrected} = 0.037$].

In the between-TD patients' subgroup analysis, the connectivity between the right caudate and the right insula was lower in medicated *v.* unmedicated patients [$t(34) = 4.77$, $p_{corrected} = 0.050$] (Fig. 2b).

No correlation between YGTSS50 and any of the connections was found in patients with TD ($p_{corrected} > 0.05$).

Discussion

Using rs-FC and a multivariate approach in a fully data-driven manner, we were able to significantly discriminate adult patients with TD from HCs, and patients with and without medication. Compared to HCs, patients with TD showed abnormal rs-FC among widespread brain areas, including striatum and cerebellum. Functional connectivity of the SMA, the OFC, the insula and the posterior parietal cortex, as well as the striatum and the cerebellum discriminated the patients under conventional medication with antipsychotics, such as aripiprazole (APZ), from the unmedicated patients. The univariate analysis found significant differences in connectivity between HCs and patients with TD within the striatum, and between medicated and unmedicated patients with TD in the connection between the caudate nucleus and the insula.
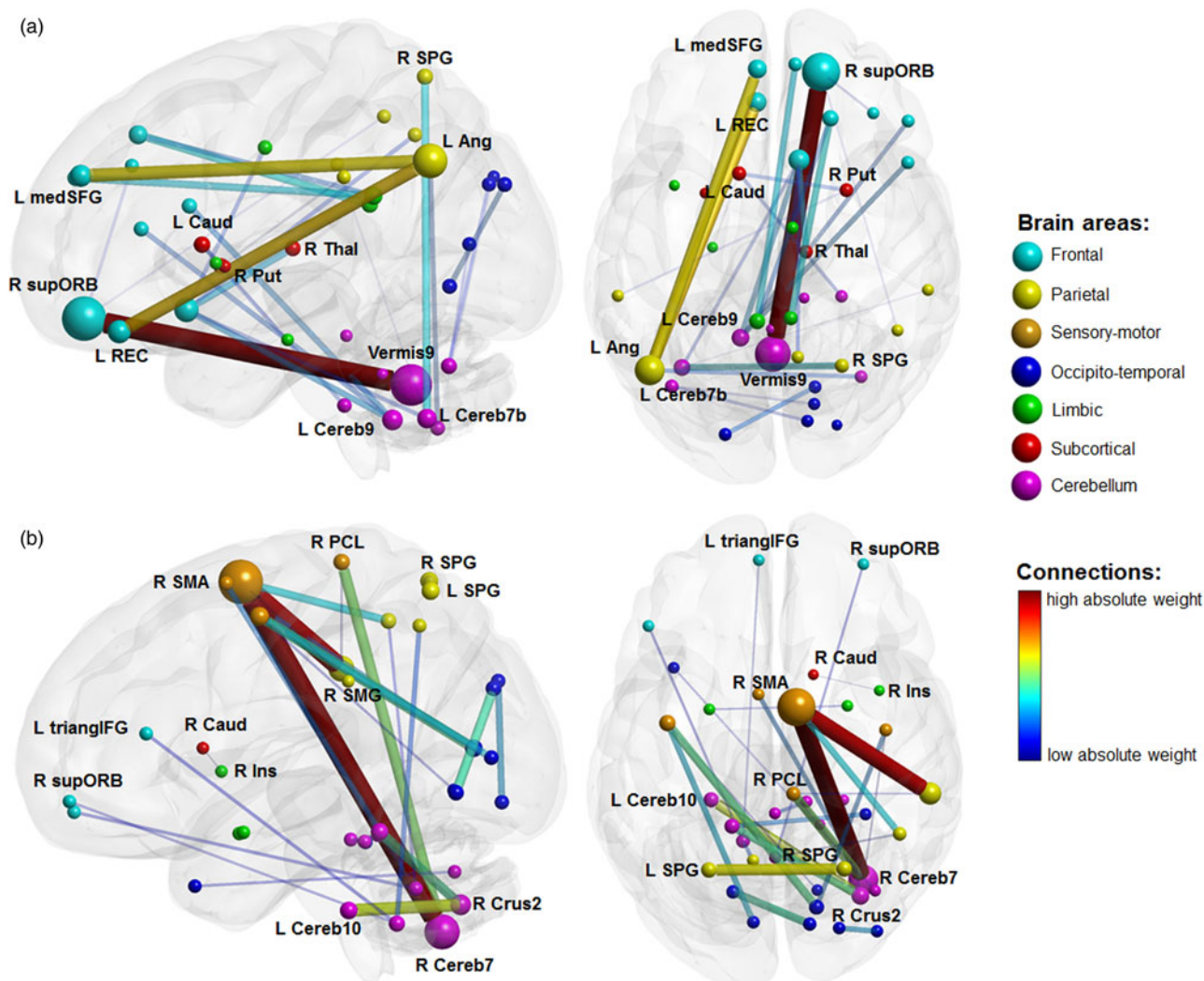
Fig. 1. SVM classifier with all HC and patients, most discriminative connections. Color code represents the absolute weights assigned to the connections. Node size represents the mean weighted number of connections entering the node over the entire set of 6670 weights. Line thickness represents the absolute mean weight of the connection over the entire set. For graphical purposes, the figure is truncated so that only the top 30 connections are displayed. (a) SVM for TD *v.* HC. (b) SVM for medicated *v.* unmedicated TD. R, right; L, left; Ang, angular gyrus; Caud, nucleus caudate; Cereb(*N*), *N*th cerebellar lobule; Ins, insula; medSFG, medial segment of the superior frontal gyrus; PCL, paracentral lobule; Put, putamen; REC, rectus gyrus; SMA, supplementary motor area; SMG, supramarginal gyrus; SPG, superior parietal gyrus; supORB, superior segment of the orbital gyrus; Thal, thalamus; triangIFG, pars triangularis of the inferior frontal gyrus.

Our study has some limitations. First, we chose the AAL atlas based on existing literature on classification of rs-FC using a similar pipeline as in our study (Lee & Frangou, 2017; Richiardi et al., 2012; Wegrzyk et al., 2018). The choice of the atlas was crucial for our approach, as the brain parcellation might have a major impact on the definition of the regions of interest, hence on the connectivity patterns, and ultimately on the results. However, previous research has compared the rs-FC classification performance across different atlases (Wegrzyk et al., 2018), and found similar accuracy of ~70% when using, for instance, the AAL, the Hammers (Hammers et al., 2003) and the Shirer (Shirer, Ryali, Rykhlevskaia, Menon, & Greicius, 2012) atlases. Second, we compared the medicated and non-medicated patients with TD in a parallel design. It is possible that patients under medication have substantial differences from the group of unmedicated patients. Thus, to fully address the question of APZ effect on brain networks, the same patients with TD should be assessed before and after the beginning of pharmacological treatment.

Overall, our results strengthen previous knowledge of altered brain networks in adult TD, and provide new evidence of specific patterns of functional connectivity in TD patients with pharmacological treatment.

Differences in functional connectivity between TD and controls

The results indicated large-scale networks' alteration in adult TD, and specifically in the connectivity between cortical areas, the cerebellum and the striatum. Other studies in patients with TD have confirmed functional and structural abnormalities between the striatum and sensory-motor cortices, OFC, parietal and temporal regions, similar to our results (Martino, Ganos, & Worbe, 2018).

The connectivity within the striatum was among the most discriminative features of our multivariate analysis. This structure, as central part of the CSTC network (Singer, 2005; Worbe, Lehericy, & Hartmann, 2015), has been suggested by various animal models
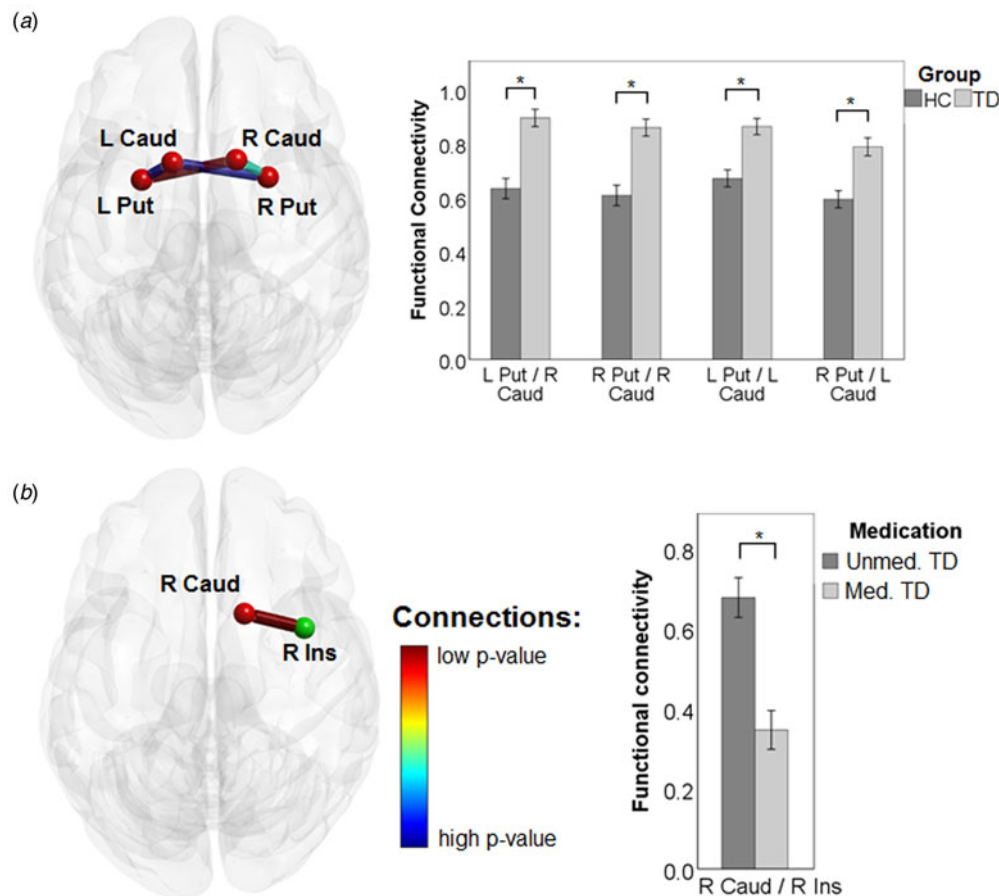
Fig. 2. Results of the univariate analysis. (a) Functional connectivity between TD and HC. (b) Functional connectivity between medicated and unmedicated TD. Bars represent the mean values ± s.ε. of the mean. * depicts significant differences at independent sample *t* tests.

to account for the wide spectrum of TD symptoms (Bronfeld, Yael, Belelovsky, & Bar-Gad, 2013; Worbe et al., 2013). Recent computational models of pathophysiology of TD have also suggested that tics and premonitory urges result from the abnormal computation of the sensation and action within sensory-motor regions of the striatum (Rae, Critchley, & Seth, 2019).

The connectivity of cerebello-cortical and cerebello-cerebellar networks was also among the most discriminative features of patients with TD compared to HCs. These results are in line with data obtained from animal models of TD, suggesting that tics result from the global neuronal rhythms abnormalities of cerebro-basal ganglia-cerebellar networks, due to striatal disinhibition (McCairn, Iriki, & Isoda, 2013). In particular, there is evidence that a cerebellar-prefrontal network is implicated in motor execution specific to Go events in Go-no-Go tasks (Mostofsky et al., 2003), and our results showed an impairment in such a network, which may lead to an alteration of unwanted movement suppression and, in turn, to tic release. Numerous studies have further confirmed abnormal structural and functional connectivity of the cerebellum with cortical areas and basal ganglia, namely the striatum (Ramkiran, Heidemeyer, Gaebler, Shah, & Neuner, 2019; Sigurdsson, Jackson, Jolley, Mitchell, & Jackson, 2020) in patients with TD.

Overall, our results point to the pivotal role of the striatum and cerebellum in the pathophysiology of TD. They also suggest that functional connectivity of the striatum, cerebello-cerebellar and

cerebello-cortical networks might be considered as potential imaging biomarkers of this disorder. However, and similar to previous research (Greene et al., 2016), SVR was not able to predict tic severity. This could result from the fact that only patients with low-to-moderate tic severity were included in the study, to guarantee the quality of MRI acquisitions. Further studies combining structural and functional connectivity are warranted to address this question. For instance, a larger hippocampal volume in children with TD predicted the persistence of tics in follow-up visits after onset (Sigurdsson et al., 2020). Moreover, our sample did not allow us to study the effects of comorbid disorders on rs-FC. Future research with a large number of patients will allow for the stratification of TD according to comorbidities, in order to disentangle their contribution to networks dysfunction. One potential limitation of this study is that we included only patients with low-to-moderate tics that did not impact the quality of the images. Also, even if the patients were not explicitly instructed to suppress their tics, some of them might have still performed this voluntary suppression, and this could have had an impact on the results.

Differences in functional connectivity between medicated and unmedicated TD

The most common drug used to treat TD in this study was APZ, taken by 83% of medicated patients. This antipsychotic acts on

the dopaminergic and serotonergic function as a partial agonist of the dopamine D2 receptor and 5-HT1A, and antagonism at 5-HT2A receptors (Jordan et al., 2004). It has shown a positive effect on tics in TD (Bubl, Perlov, & Tebartz Van Elst, 2006; Kastrup, Schlotter, Plewnia, & Bartels, 2005).

The empirical model of APZ action postulates that brain areas with high density of neurons with dopamine D2 receptors (D2R) might be more sensitive to this drug, and might, in turn, influence the activity of other regions innervated by the D2R neurons (Handley et al., 2013). Previous research has shown that, compared to placebo, APZ intake in healthy volunteers modulates activity in a network including the putamen, the insula, the caudate and the cerebellum, as well as in the superior frontal gyrus, the superior and inferior parietal lobes and the OFC (Handley et al., 2013), all regions found discriminative of medicated compared to unmedicated patients in the current study. The univariate approach pointed to differences in the connectivity between the caudate and the insula in medicated compared to unmedicated patients. The insula has been related to the 'urge-for-action' (Worbe et al., 2015), i.e. suppression of natural urges (such as blinking), in healthy participants (Lerner et al., 2009), but also to uncomfortable feeling associated with the premonitory urges in TD (Jackson, Parkinson, Kim, Schüermann, & Eickhoff, 2011). In particular, a brain network encompassing the insular cortex has been found active prior to tic onset, and concomitant with the subjective experience of the premonitory urge (Bohlhalter et al., 2006). Similarly, functional connectivity (Tinaz, Malone, Hallett, & Horovitz, 2015) and cortical thickness (Draper, Jackson, Morgan, & Jackson, 2016) of the insula have been correlated with the urge to tic in TD. Altogether, these findings support a key role of the insula in the perception of bodily urges, linking the sensory and emotional character of premonitory urges with their translation into tics (Cavanna, Black, Hallett, & Voon, 2017; Conceição, Dias, Farinha, & Maia, 2017; Cox, Seri, & Cavanna, 2018). In this study we have not monitored premonitory urges in patients with TD, however, our results indicate that antipsychotics might act on insular and striatal loops, and the tics improvement might result from premonitory urges reduction. This points to a potential effect of APZ on striatal, insular and cerebellar networks, and the activity of these areas might be used in future research to monitor the effects of medication.

One potential confound is the use of concomitant medications other than APZ, which may have an impact on rs-FC. Due to our sample size, we did not stratify according to medication type, however, most of our patients was under APZ, and our findings are in line with existing evidence of altered cortical and subcortical activity in healthy participants after APZ (Handley et al., 2013). It is, therefore, unlikely that the other drugs biased our predictions.

Overall, these results suggest that antipsychotic medication might affect the activity of areas within the CSTC loop implicated in tic generation and volitional control (Ganos, Roessner, & Münchau, 2013). Its benefic effects on these areas may, in turn, spread to other regions functionally connected to the CSTC loop, and improve other cognitive functions impaired in TD.

Advantages of multivariate approaches

The results of our study demonstrated that multivariate approaches can be successfully used to predict adult TD based on abnormal patterns of rs-FC. Recent studies have confirmed the advantage of multivariate approaches, in particular SVM, in investigating patterns of differential functional connectivity between children and adults with TD (Nielsen et al., 2020), or between children with TD and age-matched HCs (Greene et al., 2016). Yet, these studies have applied a feature reduction, and restricted the analysis to a smaller number of connections (Greene et al., 2016). Indeed, this methodological choice improves the classification accuracy and computational time, as the complexity of the model is reduced, however, it introduces a priori information on which regions carry the relevant information, often achieved through univariate comparisons (Greene et al., 2016), and might thus exclude other areas still relevant for the understanding of TD. Moreover, the interpretability of the results obtained after feature selection has been recently questioned (Nielsen et al., 2019). We opted for no feature selection, as we were interested in the connectivity at the whole-brain scale, and our classifier showed similar performance to other studies in TD (Greene et al., 2016; Nielsen et al., 2020).

Conclusions

Overall, our results showed the potential of multivariate classification methods for clinical use, to help the diagnostic process and/or to evaluate the effects of treatments. Also, the results of this study hold a promise to identify an imaging-based biomarker of TD and to monitor treatments. Future research on a larger sample will allow for accurate models in relationship with co-morbidities of TD, and will move the field closer toward imaging-based biomarkers to guide clinical decisions (Wolfers, Buitelaar, Beckmann, Franke, & Marquand, 2015).

References

American Psychological Association, A. P. (2013). *Diagnostic and statistical manual of mental disorders (DSM-5®)*. Washington, D.C, USA: American Psychiatric Pub.

Atkinson-Clement, C., Porte, C.-A., de Liege, A., Wattiez, N., Klein, Y., Beranger, B., … Pouget, P. (2020). Neural correlates and role of medication in reactive motor impulsivity in Tourette disorder. *Cortex*, *125*, 60–72.

Bohlhalter, S., Goldfine, A., Matteson, S., Garraux, G., Hanakawa, T., Kansaku, K., … Hallett, M. (2006). Neural correlates of tic generation in Tourette syndrome: An event-related functional MRI study. *Brain*, *129*(8), 2029–2037.

Bronfeld, M., Yael, D., Belelovsky, K., & Bar-Gad, I. (2013). Motor tics evoked by striatal disinhibition in the rat. *Frontiers in Systems Neuroscience*, *7*, 50.

Bubl, E., Perlov, E., & Tebartz Van Elst, L. (2006). Aripiprazole in patients with Tourette syndrome. *The World Journal of Biological Psychiatry*, *7*(2), 123–125.

Cavanna, A. E., Black, K. J., Hallett, M., & Voon, V. (2017). Neurobiology of the premonitory urge in Tourette's syndrome: Pathophysiology and treatment implications. *The Journal of Neuropsychiatry and Clinical Neurosciences*, 29(2), 95–104.

Conceição, V. A., Dias, Â, Farinha, A. C., & Maia, T. V. (2017). Premonitory urges and tics in Tourette syndrome: Computational mechanisms and neural correlates. *Current Opinion in Neurobiology*, 46, 187–199.

Cox, J. H., Seri, S., & Cavanna, A. E. (2018). Sensory aspects of Tourette syndrome. *Neuroscience & Biobehavioral Reviews*, 88, 170–176.

Draper, A., Jackson, G. M., Morgan, P. S., & Jackson, S. R. (2016). Premonitory urges are associated with decreased grey matter thickness within the insula and sensorimotor cortex in young people with Tourette syndrome. *Journal of Neuropsychology*, 10(1), 143–153.

Eddy, C. M., Cavanna, A. E., Rickards, H. E., & Hansen, P. C. (2016). Temporo-parietal dysfunction in Tourette syndrome: Insights from an fMRI study of theory of mind. *Journal of Psychiatric Research*, 81, 102–111.

Fahim, C., Yoon, U., Das, S., Lyttelton, O., Chen, J., Arnaoutelis, R., … Brandner, C. (2010). Somatosensory–motor bodily representation cortical thinning in Tourette: Effects of tic severity, age and gender. *Cortex*, 46(6), 750–760.

Fredericksen, K., Cutting, L., Kates, W., Mostofsky, S. H., Singer, H., Cooper, K., … Kaufmann, W. E. (2002). Disproportionate increases of white matter in right frontal lobe in Tourette syndrome. *Neurology*, 58(1), 85–89.

Ganos, C., Roessner, V., & Münchau, A. (2013). The functional anatomy of Gilles de la Tourette syndrome. *Neuroscience & Biobehavioral Reviews*, 37(6), 1050–1062.

Greene, D. J., Church, J. A., Dosenbach, N. U., Nielsen, A. N., Adeyemo, B., Nardos, B., … Schlaggar, B. L. (2016). Multivariate pattern classification of pediatric Tourette syndrome using functional connectivity MRI. *Developmental Science*, 19(4), 581–598.

Hammers, A., Allom, R., Koepp, M. J., Free, S. L., Myers, R., Lemieux, L., … Duncan, J. S. (2003). Three-dimensional maximum probability atlas of the human brain, with particular reference to the temporal lobe. *Human Brain Mapping*, 19(4), 224–247.

Handley, R., Zelaya, F. O., Reinders, A. S., Marques, T. R., Mehta, M. A., O'Gorman, R., … Williams, S. (2013). Acute effects of single-dose aripiprazole and haloperidol on resting cerebral blood flow (rCBF) in the human brain. *Human Brain Mapping*, 34(2), 272–282.

Hastie, T., Tibshirani, R., & Friedman, J. (2009). *The elements of statistical learning: Data mining, inference, and prediction*. Washington, D.C, USA: Springer Science & Business Media.

Hirschtritt, M. E., Lee, P. C., Pauls, D. L., Dion, Y., Grados, M. A., Illmann, C., … Lyon, G. J. (2015). Lifetime prevalence, age of risk, and genetic relationships of comorbid psychiatric disorders in Tourette syndrome. *JAMA Psychiatry*, 72(4), 325–333.

Jackson, S. R., Parkinson, A., Kim, S. Y., Schüermann, M., & Eickhoff, S. B. (2011). On the functional anatomy of the urge-for-action. *Cognitive Neuroscience*, 2(3–4), 227–243.

Jenkinson, M., Beckmann, C. F., Behrens, T. E., Woolrich, M. W., & Smith, S. M. (2012). FSL. *Neuroimage*, 62(2), 782–790.

Jordan, S., Koprivica, V., Dunn, R., Tottori, K., Kikuchi, T., & Altar, C. A. (2004). In vivo effects of aripiprazole on cortical and striatal dopaminergic and serotonergic function. *European Journal of Pharmacology*, 483(1), 45–53.

Kastrup, A., Schlotter, W., Plewnia, C., & Bartels, M. (2005). Treatment of tics in Tourette syndrome with aripiprazole. *Journal of Clinical Psychopharmacology*, 25(1), 94–96.

Kates, W. R., Frederikse, M., Mostofsky, S. H., Folley, B. S., Cooper, K., Mazur-Hopkins, P., … Pearlson, G. D. (2002). MRI Parcellation of the frontal lobe in boys with attention deficit hyperactivity disorder or Tourette syndrome. *Psychiatry Research: Neuroimaging*, 116(1–2), 63–81.

Kundu, P., Inati, S. J., Evans, J. W., Luh, W.-M., & Bandettini, P. A. (2012). Differentiating BOLD and non-BOLD signals in fMRI time series using multi-echo EPI. *Neuroimage*, 60(3), 1759–1770.

Kundu, P., Voon, V., Balchandani, P., Lombardo, M. V., Poser, B. A., & Bandettini, P. A. (2017). Multi-echo fMRI: A review of applications in fMRI denoising and analysis of BOLD signals. *Neuroimage*, 154, 59–80.

Leckman, J. F., Riddle, M. A., Hardin, M. T., Ort, S. I., Swartz, K. L., Stevenson, J., & Cohen, D. J. (1989). The Yale global tic severity scale: Initial testing of a clinician-rated scale of tic severity. *Journal of the American Academy of Child & Adolescent Psychiatry*, 28(4), 566–573.

Lee, W. H., & Frangou, S. (2017). Linking functional connectivity and dynamic properties of resting-state networks. *Scientific Reports*, 7(1), 1–10.

Lerner, A., Bagic, A., Boudreau, E., Hanakawa, T., Pagan, F., Mari, Z., … Simmons, J. (2007). Neuroimaging of neuronal circuits involved in tic generation in patients with Tourette syndrome. *Neurology*, 68(23), 1979–1987.

Lerner, A., Bagic, A., Hanakawa, T., Boudreau, E. A., Pagan, F., Mari, Z., … Murphy, D. L. (2009). Involvement of insula and cingulate cortices in control and suppression of natural urges. *Cerebral Cortex*, 19(1), 218–223.

Marques, J. Retrieved from https://github.com/JosePMarques/MP2RAGE-related-scripts.

Martino, D., Ganos, C., & Worbe, Y. (2018). Neuroimaging applications in Tourette's syndrome. *International Review of Neurobiology*, 143, 65–108.

Mazzone, L., Yu, S., Blair, C., Gunter, B. C., Wang, Z., Marsh, R., & Peterson, B. S. (2010). An FMRI study of frontostriatal circuits during the inhibition of eye blinking in persons with Tourette syndrome. *American Journal of Psychiatry*, 167(3), 341–349.

McCairn, K. W., Iriki, A., & Isoda, M. (2013). Global dysrhythmia of cerebro-basal ganglia–cerebellar networks underlies motor tics following striatal disinhibition. *Journal of Neuroscience*, 33(2), 697–708.

Mostofsky, S. H., Schafer, J. G., Abrams, M. T., Goldberg, M. C., Flower, A. A., Boyce, A., … Denckla, M. B. (2003). fMRI evidence that the neural basis of response inhibition is task-dependent. *Cognitive Brain Research*, 17(2), 419–430.

Nielsen, A. N., Barch, D. M., Petersen, S. E., Schlaggar, B. L., & Greene, D. J. (2019). Machine learning with neuroimaging: Evaluating its applications in psychiatry. *Biological Psychiatry: Cognitive Neuroscience and Neuroimaging*, 5, 791–798.

Nielsen, A. N., Gratton, C., Church, J. A., Dosenbach, N. U., Black, K. J., Petersen, S. E., … Greene, D. J. (2020). Atypical functional connectivity in Tourette syndrome differs between children and adults. *Biological Psychiatry*, 87(2), 164–173.

O'Brien, K. R., Kober, T., Hagmann, P., Maeder, P., Marques, J., Lazeyras, F., … Roche, A. (2014). Robust T1-weighted structural brain imaging and morphometry at 7T using MP2RAGE. *PLoS One*, 9(6), e99676 (online journal).

Power, J. D., Mitra, A., Laumann, T. O., Snyder, A. Z., Schlaggar, B. L., & Petersen, S. E. (2014). Methods to detect, characterize, and remove motion artifact in resting state fMRI. *Neuroimage*, 84, 320–341.

Rae, C. L., Critchley, H. D., & Seth, A. K. (2019). A Bayesian account of the sensory-motor interactions underlying symptoms of Tourette syndrome. *Frontiers in Psychiatry*, 10, 29.

Ramkiran, S., Heidemeyer, L., Gaebler, A., Shah, N. J., & Neuner, I. (2019). Alterations in basal ganglia-cerebello-thalamo-cortical connectivity and whole brain functional network topology in Tourette's syndrome. *NeuroImage: Clinical*, 24, 101998.

Richiardi, J., Gschwind, M., Simioni, S., Annoni, J.-M., Greco, B., Hagmann, P., … Van De Ville, D. (2012). Classifying minimally disabled multiple sclerosis patients from resting state functional connectivity. *Neuroimage*, 62(3), 2021–2033.

Shirer, W. R., Ryali, S., Rykhlevskaia, E., Menon, V., & Greicius, M. D. (2012). Decoding subject-driven cognitive states with whole-brain connectivity patterns. *Cerebral Cortex*, 22(1), 158–165.

Sigurdsson, H. P., Jackson, S. R., Jolley, L., Mitchell, E., & Jackson, G. M. (2020). Alterations in cerebellar grey matter structure and covariance networks in young people with Tourette syndrome. *Cortex*, 126, 1–15.

Singer, H. S. (2005). Tourette's syndrome: From behaviour to biology. *The Lancet Neurology*, 4(3), 149–159.

Tinaz, S., Malone, P., Hallett, M., & Horovitz, S. G. (2015). Role of the right dorsal anterior insula in the urge to tic in Tourette syndrome. *Movement Disorders*, 30(9), 1190–1197.

Tzourio-Mazoyer, N., Landeau, B., Papathanassiou, D., Crivello, F., Etard, O., Delcroix, N., … Joliot, M. (2002). Automated anatomical labeling of activations in SPM using a macroscopic anatomical parcellation of the MNI MRI single-subject brain. *Neuroimage*, 15(1), 273–289.

Wegrzyk, J., Kebets, V., Richiardi, J., Galli, S., Van de Ville, D., & Aybek, S. (2018). Identifying motor functional neurological disorder using resting-state functional connectivity. *NeuroImage: Clinical*, 17, 163–168.

Wolfers, T., Buitelaar, J. K., Beckmann, C. F., Franke, B., & Marquand, A. F. (2015). From estimating activation locality to predicting disorder: A review of pattern recognition for neuroimaging-based psychiatric diagnostics. *Neuroscience & Biobehavioral Reviews*, 57, 328–349.

Worbe, Y., Gerardin, E., Hartmann, A., Valabrégue, R., Chupin, M., Tremblay, L., … Lehéricy, S. (2010). Distinct structural changes underpin clinical phenotypes in patients with Gilles de la Tourette syndrome. *Brain*, 133(12), 3649–3660.

Worbe, Y., Lehericy, S., & Hartmann, A. (2015). Neuroimaging of tic genesis: Present status and future perspectives. *Movement Disorders*, 30(9), 1179–1183.

Worbe, Y., Malherbe, C., Hartmann, A., Pélégrini-Issac, M., Messé, A., Vidailhet, M., … Benali, H. (2012). Functional immaturity of cortico-basal ganglia networks in Gilles de la Tourette syndrome. *Brain*, 135(6), 1937–1946.

Worbe, Y., Sgambato-Faure, V., Epinat, J., Chaigneau, M., Tandé, D., François, C., … Tremblay, L. (2013). Towards a primate model of Gilles de la Tourette syndrome: Anatomo-behavioural correlation of disorders induced by striatal dysfunction. *Cortex*, 49(4), 1126–1140.

Wu, G., & Chang, E. Y. (2003). Class-boundary alignment for imbalanced dataset learning. Paper presented at the ICML 2003 workshop on learning from imbalanced data sets II, Washington, DC.